Thermal, Magnetic, and Structural Characterization of the Crystallization Kinetics of Amorphous Soft Magnetic Materials

A. Hsiao,[1] C. Ashe,[1] M. E. McHenry,[1] M. J. Kramer[2]
[1]Department of Materials Science and Engineering, Carnegie Mellon University (CMU), Pittsburgh, PA, U.S.A.
[2]Ames Laboratory and Department of Materials Science and Engineering, Iowa State University, Ames, IA, U.S.A.

Introduction

An understanding of the crystallization kinetics of magnetic amorphous alloys is of scientific interest for two important reasons. First, for an alloy that exhibits excellent magnetic properties in its amorphous phase, the crystallization kinetics represent the limit at which these properties begin to deteriorate. Therefore, thermal stability determines the magnetic stability of the amorphous phase of the material. Second, for an alloy that exhibits excellent magnetic properties in its two-phase, nanocrystal-amorphous matrix structure, control over the crystallization kinetics provides the ability to tailor microstructure. The amount of nanocrystals formed within the matrix can be controlled to achieve the desired magnetic performance. The modes of crystallization — from the metastable amorphous state to the stable crystalline state — depend on various parameters, such as composition, concentration of nucleation sites, diffusion coefficients, activation energy for diffusion, free energy difference between amorphous and crystalline phases, and thermal history of the sample.

Methods and Materials

Six sets of NANOPERM™ ribbon were prepared, each with a weight of 10 ±2 mg. A heating rate was assigned to each sample, resulting in six different heating rates to be tested: 2°, 5°, 10°, 20°, 40°, and 60°C/min. Each sample was heated from 50° to 580°C. It was shown that the peak temperature T_p increases as the heating rate increases [1], suggesting a dependence of T_p on the heating rate of the sample. The temperature dependence of T_p on the heating rate demonstrates that the Kissinger model of transformation can be used to relate the rate of heating to the activation energy and temperature. The activation energy from the Kissinger model was calculated to be 3.4 eV. This is the fitted value for the slope of a Kissinger plot, where the regression coefficient was $R^2 = 0.999$. These same samples were then subjected to *in situ* crystallization in a vibrating sample magnetometer (VSM). As the alloy crystallizes, the magnetization is directly proportional to the volume fraction of bcc α-Fe that forms. Thus, the volume fraction transformed can be determined as a fraction of time, since it is directly related to the magnetization of the sample. Table 1 summarizes the values of morphology index **n** and rate constant **k** at different time constants for NLR fits at 490°, 500°, 510°, and 520°C. The NLR fits to isothermal data at 570° and 550°C were imprecise (R^2 of <0.97) and resulted in inconsistent values of (n). Therefore, the reactions at 570° and 550°C were determined to occur too quickly for the data to be included in the collective analysis. It can be seen from the table that the best nonlinear regression fit for these four isothermal experiments occurs for a time constant of $\tau = 120$ s.

While thermal analysis and magnetometry are excellent techniques for indirectly measuring the crystal structure evolution, x-ray diffraction is a more direct approach. Synchrotron radiation has been shown to be an excellent source for high-resolution powder diffraction studies. By using a newly designed high-temperature furnace coupled with a sample rotation apparatus [2], changes in the diffraction pattern are obtained in real time, corresponding to the phase transformations that occur during the crystallization process. As a result, the amorphous-to-crystalline transition is clearly observed by this method, as well as are the appearance and identification of nanocrystalline phases.

Table 1. Kinetic parameters from nonlinear regression analysis of JMA isothermal data on NANOPERM.

	Temperature (°C)			
	490	500	510	520
τ (s)	Morphology index (n)			
0	1.95	1.68	1.27	1.79
90	1.88	1.58	1.13	1.52
120	1.85	1.55	1.08	1.43
150	1.81	1.48	X	X
180	1.80	1.48	X	X
210	1.77	1.45	X	X
421	1.56	X	X	X
	Rate constant (k)			
0	3.2×10^{-4}	5.0×10^{-4}	8.6×10^{-4}	1.2×10^{-3}
90	3.3×10^{-4}	5.0×10^{-4}	9.4×10^{-4}	1.4×10^{-3}
120	3.0×10^{-4}	5.0×10^{-4}	9.7×10^{-4}	1.4×10^{-3}
150	3.3×10^{-4}	5.1×10^{-4}	X	X
180	3.3×10^{-4}	5.2×10^{-4}	X	X
210	3.4×10^{-4}	5.3×10^{-4}	X	X
421	3.7×10^{-4}	X	X	X

Results

Figure 1 illustrates the characteristics of the crystallization transformations of NANOPERM ribbon: (1) the sharpening of the Fe(110) peak is apparent as the transformation of the amorphous to the crystalline phase occurs; (2) primary crystallization of α-Fe is confirmed with the appearance of the Fe(200) peak at T_{x1} of ~510°C; (3) the shape of the increase of the intensity peak of Fe(110) is precisely the shape of the trend from Scherrer analysis of the Fe(200) peak shown in Fig. 2; and (4) T_{x2} occurs at ~710°C with the crystallization of $Fe_{23}Zr_6$.

Figure 2 shows the size of the nanocrystals as a function of temperature, from Scherrer analysis. The slope of the change in crystalline size increases after T_{x1}, indicating crystallization and growth of α-Fe. This growth begins to plateau near 700°C, possibly attributed to the formation of a Zr-rich amorphous phase surrounding each α-Fe particle as Zr is expelled from the α-Fe to the intergranular region. At the secondary crystallization event, $Fe_{23}Zr_6$ forms from the Zr-rich interphase phase, and Zr is no longer a barrier. The slope of the volume fraction transformed increases above 700°C.

Secondary crystallization of $Fe_{23}Zr_6$ is seen in Fig. 3. Well after T_{x2} of ~715°C, distinct peaks of $Fe_{23}Zr_6$ appear. These peaks are not present below T_{x2}. The appearance of $Fe_{23}Zr_6$ instead of Fe_3Zr confirms the nonequilibrium characteristic of crystallization.

Discussion

The activation energy for Fe self-diffusion in pure bcc α-Fe is 239.7 kJ/mole or 2.5 eV at atmospheric pressure [3]. However, it can be seen from the experimentally determined higher values of activation energy in both the isothermal and constant-heating kinetics that Zr and B also play a part in the crystallization of NANOPERM. Indeed, Zr also diffuses away from the growing crystals. (Activation energy for substitutional self-diffusion of β-Zr is 273.5 kJ/mol or 2.8 eV.) From the various analyses presented here, the morphology index is concluded to be n = 3/2 for NANOPERM, where the reaction is three-dimensionally diffusion-limited after initial, immediate nucleation. Values of Q and n are comparable to those published in the literature on similar amorphous magnetic alloys.

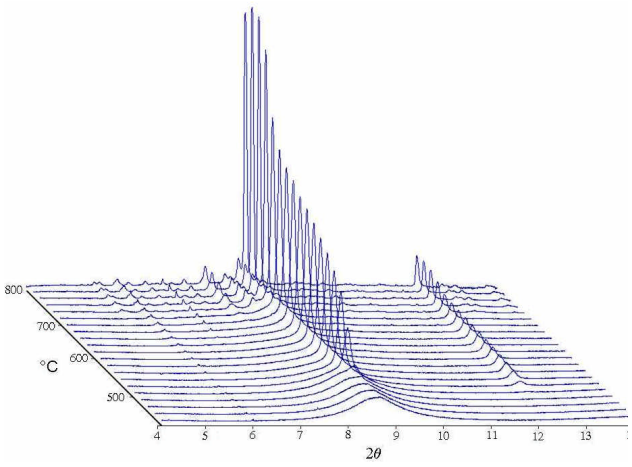

FIG. 1. 3-D synchrotron diffraction patterns of α-Fe from 400° to 800°C, showing the transformation from amorphous to crystalline, first and second crystallization phases, and the growth and coarsening phenomena of NANOPERM crystallization kinetics.

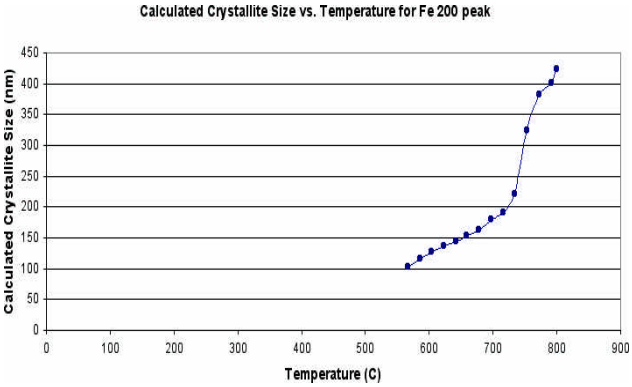

FIG. 2. Scherrer analysis of a Fe(200) x-ray diffraction peak vs. temperature.

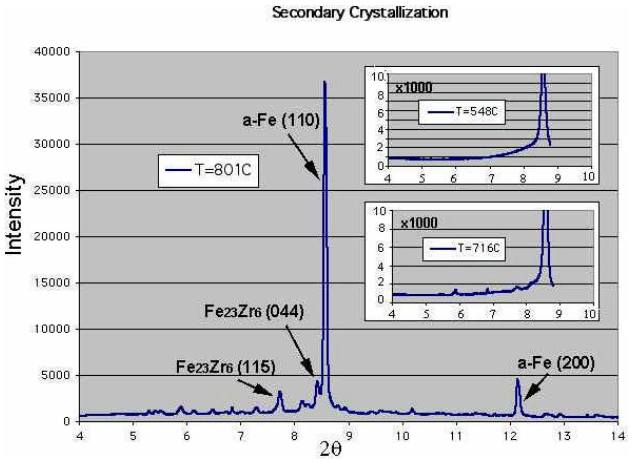

FIG. 3. Synchrotron radiation diffraction pattern of secondary crystallization of $Fe_{23}Zr_6$ of NANOPERM. At 546°C, only sharp intensity peaks are present for α-Fe. The onset of secondary crystallization occurs at 716°C.

Acknowledgments

The work at Ames Laboratory was supported by the U.S. Department of Energy (DOE), Office of Science, Office of Basic Energy Sciences (BES), through Iowa

State University under Contract W-7405-ENG-82. Work at CMU was supported by the National Science Foundation through Grant Award DMR-9803700, by the Air Force Office of Scientific Research, Air Force Material Command, USAF, under Grant No. 49620-96-1-0454, and by ABB Corporation. The Midwest Universities Collaborative Access Team (MU-CAT) sector at the APS is supported by the DOE BES through Ames Laboratory under Contract No. W-7405-ENG-82. Use of the APS was supported by the DOE BES under Contract No. W-31-109-ENG-38.

References

[1] A. Hsiao, Z. Turgut, M. A. Willard, E. Selinger, D. E. Laughlin, M. E. McHenry, and R. Hasagawa, MRS Symp. Proc. **577**, 551-556 (1999).

[2] M. J. Kramer, L. Margulies, and R. W. McCallum, Rev. Sci. Instrum. **70**(9), 3554-3561 (1999).

[3] D. A. Porter and K. E. Easterling, *Phase Transformations in Metals and Alloys*, 2nd ed. (Chapman & Hall, London, 1992), p. 78.